



# City Research Online

## City, University of London Institutional Repository

---

**Citation:** Kappos, A. J. (2013). Seismic Vulnerability and Loss Assessment for Buildings in Greece. In: Gueguen, P. (Ed.), Seismic Vulnerability of Structures. (pp. 111-159). Wiley-ISTE. ISBN 1118603966

This is the accepted version of the paper.

This version of the publication may differ from the final published version.

---

**Permanent repository link:** <https://openaccess.city.ac.uk/id/eprint/12756/>

**Link to published version:** <http://dx.doi.org/10.1002/9781118603925.ch3>

**Copyright:** City Research Online aims to make research outputs of City, University of London available to a wider audience. Copyright and Moral Rights remain with the author(s) and/or copyright holders. URLs from City Research Online may be freely distributed and linked to.

**Reuse:** Copies of full items can be used for personal research or study, educational, or not-for-profit purposes without prior permission or charge. Provided that the authors, title and full bibliographic details are credited, a hyperlink and/or URL is given for the original metadata page and the content is not changed in any way.

# Seismic vulnerability and loss assessment for buildings in Greece

**Andreas J. Kappos**

Aristotle University of Thessaloniki, Dept of Civil Engineering

## 1 Introduction

This chapter describes the methodology for seismic vulnerability assessment developed at the Aristotle University of Thessaloniki (AUPh), which is based on the so-called ‘hybrid’ approach. The basic feature of this approach is that it combines statistical data with appropriately processed (utilising repair cost models) results from nonlinear dynamic or static analyses, that permit extrapolation of statistical data to PGA's and/or spectral displacements for which no data is available. The statistical data sets used herein are from earthquake-damaged Greek buildings. The chapter focuses on the derivation of vulnerability (fragility) curves in terms of peak ground acceleration (PGA), as well as spectral displacement ( $S_d$ ), and also includes the estimation of capacity curves ( $S_a$  vs.  $S_d$  diagrams), for several reinforced concrete (R/C) and unreinforced (load-bearing) masonry (URM) building types common in Greece as well as the rest of Southern Europe.

The numerical studies involved in the development of the aforementioned ‘hybrid’ fragility curves included modelling and analysis of a large number of building types, representing most of the common typologies in S. Europe. Building classes were defined on the basis of material, structural system, height, and age (which indirectly defines also the code used for design, if any), and, in the case of R/C buildings, the existence or otherwise of brick masonry infills. The R/C building models were analysed for a set of carefully selected accelerograms representative of different ground conditions. The results of all these inelastic response-history analyses were used for developing the so-called ‘primary’ vulnerability curves, i.e. plots of the evolution of the selected damage index (e.g. the monetary loss) as a function of the earthquake intensity. Critical in this respect is the way structural damage indices calculated in analysis are translated into loss, using appropriate empirical relationships. The next steps consist in defining a number of damage states (described in terms of e.g. the loss index), assuming a certain probabilistic model for the fragility (e.g. lognormal), and deriving probabilistic vulnerability, i.e. fragility, curves for each building typology. These curves were also used, in combination with appropriately defined response spectra, for the derivation of alternative fragility curves involving spectral quantities ( $S_d$ ).

The chapter also presents another approach based on inelastic static analysis, which is more suitable for structures that are not particularly amenable to nonlinear response-history analysis, such as the URM buildings. In this approach ‘pushover’ (or ‘resistance’) curves are derived for all building types (R/C and URM), then reduced to standard capacity curves ( $S_a$  vs.  $S_d$ ), and can be used together with the  $S_d$ -based fragility curves as an alternative to the aforementioned curves in loss assessment or in developing earthquake scenarios.

The last part of the chapter is devoted to the application of the fragility curve methodology for deriving an earthquake scenario for the building stock of the municipality of Thessaloniki. By ‘scenario’ it is understood here that the study refers to a given earthquake and provides a

comprehensive description of what happens when such an earthquake occurs; this is not the same as ‘risk analysis’ that refers to all the possible arriving earthquakes, estimating the probability of losses over a specified period of time. It is notable that the last 15 years have witnessed a growing interest in assessing the seismic vulnerability of European cities and the associated risk. Several earthquake damage (and loss) scenario studies appeared wherein some of the most advanced techniques have been applied to the urban habitat of European cities (Barbat et al. 1996, Bard et al. 1995, D’Ayala et al. 1996, Dolce et al. 2006, Erdik et al. 2003, Faccioli et al. 1999, Kappos et al. 2002, 2008, 2010). A key feature of the most recent among these studies, including the one presented here for Thessaloniki, is the use of advanced GIS tools that permit clear representation of the expected distribution of damage in the studied area and visualisation of the effects of any risk mitigation strategy that can be adopted on the basis of the scenario.

## 2 Vulnerability assessment of R/C buildings

### 2.1 Buildings Analysed

Using the procedures described in the following, analysis of several different R/C building configurations has been performed, representing practically all common R/C building types in Greece and several other S. European countries. Referring to the height of the buildings, 2-storey, 4-storey, and 9-storey R/C buildings were selected as representative of Low-rise, Medium-rise and High-rise, respectively. The nomenclature used for the buildings is of the type RC<sub>ixy</sub> where *i* indicates the structural system, *x* the height and *y* the code level. Regarding the structural system, both frames (RC1 and RC3 types) and dual (frame+shear wall) systems were addressed (RC4). Each of the above buildings was assumed to have three different configurations, ‘bare’ (without masonry infill walls, RC1 type), ‘regularly infilled’ (RC3.1) and ‘irregularly infilled’ (soft ground storey, usually pilotis, RC3.2 type).

Regarding the level of seismic design and detailing, four subclasses could be defined, as follows:

- *No code* (or pre-code): R/C buildings with very low level of seismic design or no seismic design at all, and poor quality of detailing of critical elements; e.g. RC1MN (medium-rise, no code).
- *Low code*: R/C buildings with low level of seismic design (roughly corresponding to pre-1980 codes in S. Europe, e.g. the 1959 Code for Greece); e.g. RC3.2LL (low-rise, low code).
- *Moderate code*: R/C buildings with medium level of seismic design (roughly corresponding to post-1980 codes in S. Europe, e.g. the 1985 Supplementary Clauses of the Greek Seismic Codes) and reasonable seismic detailing of R/C members; e.g. RC3.1HM (high-rise, moderate code).
- *High code*: R/C buildings with enhanced level of seismic design and ductile seismic detailing of R/C members according to the new generation of seismic codes (similar to Eurocode 8).

The available statistical data was not sufficient for distinguishing between all four sub-categories of seismic design. Moreover, analysis of the damage statistics for Thessaloniki buildings after the 1978 Volvi earthquake (Penelis et al. 1989) has clearly shown that there was no reduction in the vulnerability of R/C buildings following the introduction of the first (rather primitive by today’s standards) seismic code in 1959. Even if this is not necessarily the

case in all cities, differentiation between RCixN and RCixL, as well as between RCixM and RCixH is difficult, and judgement and/or code-type approaches are used to this effect. Three sets of analyses were finally carried out, for three distinct levels of design, ‘L’ (buildings up to 1985), ‘M’ (1986-1995), and ‘H’, the last one corresponding to buildings designed to the 1995 and 2000 (EAK) Greek Codes. The 1995 code (‘NEAK’) was the first truly modern seismic code (quite similar to Eurocode 8) introduced in Greece and its differences from EAK2000 are minor and deemed not to affect the vulnerability of the buildings; hence buildings constructed from 1996 to date are classified as ‘H’. Differences (in terms of strength and available ductility) between ‘N’ and ‘L’ buildings, and ‘M’ and ‘H’ buildings are addressed in a semi-empirical way at the level of capacity curves (section 2.4).

## 2.2 Inelastic analysis procedure

For all Low, Moderate, and High code R/C buildings inelastic static and dynamic time-history analyses were carried out using the SAP2000N (Computers & Structures 2002) and the in-house software DRAIN2000, respectively. R/C members were modelled using lumped plasticity beam-column elements, while infill walls were modelled using the diagonal strut element for the inelastic static analyses, and the shear panel isoparametric element for the inelastic dynamic analyses, as developed in previous studies (Kappos et al. 1998a).

In total 72 structures were addressed in this study, but full analyses were carried out for 54 of them (N and L buildings were initially considered together, as discussed previously, but different pushover curves were finally drawn, see section 2.3). To keep the cost of analysis within reasonable limits, all buildings were analysed as 2D structures. One of the typical structures studied is shown in figure 1. It is pointed out that although the consideration of 2D models means that effects like torsion due to irregularity in plan were ignored, previous studies (Kappos et al. 1998b) have shown that the entire analytical model (which also comprises the structural damage vs. loss relationship) slightly underpredicts the actual losses of the 1978 Thessaloniki earthquake, from which the statistical damage data used in the hybrid procedure originate. Moreover, evaluation of that actual damage data has shown (Penelis et al. 1989) that plan irregularities due to unsymmetric arrangement of masonry infills were far less influential than irregularities in elevation (soft storeys due to discontinuous arrangement of infills); the latter are directly taken into account in the adopted analytical models.

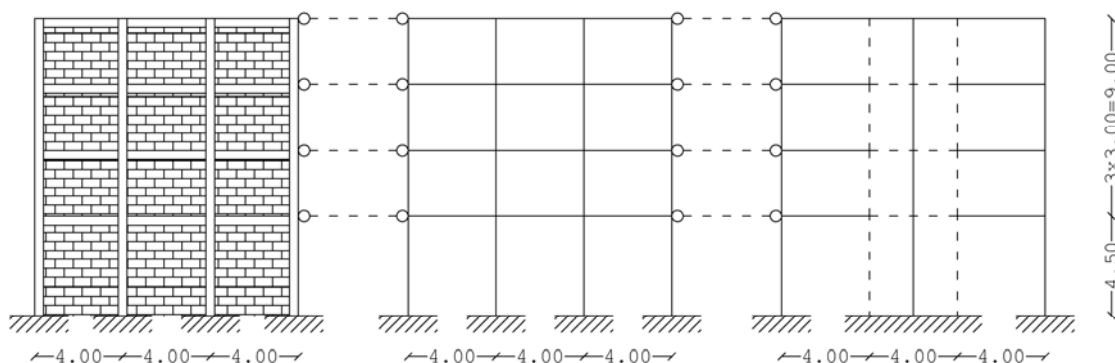


Figure 1. Four-storey, regularly infilled, R/C building with dual system (RC4.2M type).

Using the DRAIN2000 code, inelastic dynamic time-history analyses were carried out for each building type and for records scaled to several PGA values, until ‘failure’ was detected. A total of 16 accelerograms was used (to account for differences in the spectral characteristics of the ground motion), scaled to each PGA value, hence resulting to several thousands of inelastic time-history analyses (the pseudo-acceleration spectra of the 16 records are shown in figure 2). The 8 recorded motions are: 4 from the 1999 Athens earthquake (A299\_T, A399\_L, A399\_T, A499\_L), 2 from the 1995 Aegion earthquake (aigx, aigy) and 2 from the 2003 Lefkada earthquake. The 8 synthetic motions are calculated for Volos (A4, B1, C1, D1), and Thessaloniki (I20\_855, N31\_855, I20\_KOZ, N31\_KOZ) sites (as part of microzonation studies).

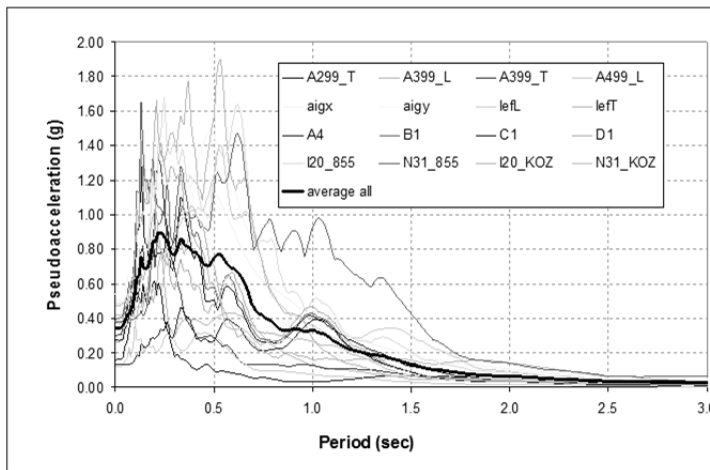


Figure 2. Pseudoacceleration spectra of the 16 motions used for the inelastic dynamic analyses.

### 2.3 Estimation of economic loss using inelastic dynamic analysis

From each analysis, the cost of repair (which is less than or equal to the replacement cost) is estimated for the building type analysed, using the models for member damage indices proposed by Kappos et al. (1998b). The total loss for the entire building is derived from empirical equations (calibrated against cost of damage data from Greece)

$$L = 0.25D_c + 0.08D_p \quad (\leq 5 \text{ storeys}) \quad (1a)$$

$$L = 0.30 D_c + 0.08D_p \quad (6 - 10 \text{ storeys}) \quad (1b)$$

where  $D_c$  and  $D_p$  are the global damage indices ( $\leq 1$ ) for the R/C members and the masonry infills of the building, respectively. Due to the fact that the cost of the R/C structural system and the infills totals less than 40% of the cost of a (new) building, the above relationships give values up to 38% for the loss index  $L$ , wherein replacement cost refers to the entire building. In the absence of a more exact model, situations leading to the need for replacement (rather than repair/strengthening) of the building are identified using *failure criteria* for members and/or storeys, as follows:

- In R/C *frame* structures (RC1 and RC3 typology), failure is assumed to occur (and then  $L=1$ ) whenever *either* 50% or more of the columns in a storey ‘fail’ (i.e. their plastic rotation capacity is less than the corresponding demand calculated from the inelastic analysis), *or* the interstorey drift exceeds a value of 4% at any storey (Dymiotis et al. 1999).

- In R/C *dual* structures (RC4 typology), failure is assumed to occur (and then  $L=1$ ) whenever *either* 50% or more of the columns in a storey ‘fail’, *or* the walls (which carry most of the lateral load) in a storey fail, *or* the interstorey drift exceeds a value of 2% at any storey (drifts at failure are substantially lower in systems with R/C walls).

This set of failure criteria was proposed by Kappos et al. (2006); they resulted after evaluating a large number of inelastic time-history analyses. Although they represent the author’s best judgement (for an analysis of the type considered herein), it must be kept in mind that situations close to failure are particularly difficult to model, and all available procedures have some limitations. For instance, although in most cases the earthquake intensity estimated to correspond to failure (damage state 5 in Table 2) is of a reasonable magnitude, in some cases (in particular wall/dual structures, especially if designed to modern codes) PGAs associated with failure are unrealistically high and should be revised in future studies. Having said this, their influence in a risk analysis is typically limited, since the scenario earthquakes do not lead to accelerations more than about  $1g$ .

## 2.4 Development of pushover and capacity curves

A resistance curve (wherein resistance encompasses both strength and ductility), also called pushover curve, is a plot of a building’s lateral load resistance as a function of a characteristic lateral displacement (typically a base shear vs. top displacement curve) derived from inelastic static (pushover) analysis. In order to facilitate direct comparison with spectral demand, base shear is converted to spectral acceleration and the roof displacement is converted to spectral displacement using modal properties and the equivalent SDOF system approach, resulting in a ‘capacity curve’ in terms of spectral quantities (e.g. FEMA-NIBS 2003).

Pushover analyses were carried out for all Low-Code, Moderate-Code, and High-Code building models. No-code (or Pre-Code) buildings were assumed to have 20% lower strength than Low Code ones, but the same displacement ductility factor ( $S_{du}/S_{dy}$ ), reflecting the well-established fact that in Greece ductility was not an issue in seismic design prior to the 1985 revision of the Seismic Code.

Some typical pushover curves and their corresponding bilinear versions (derived on the basis of equal areas under the curves) are given in Figure 3; as shown in the figure, the equal areas are calculated up to the point where the first significant drop in strength (usually about 20%) occurs in the ‘complete’ pushover curve.

Building capacity curves are constructed for each model building type and represent different levels of seismic design level and building performance. Each curve is defined by two points: (1) the ‘yield’ capacity and (2) the ‘ultimate’ capacity. The yield capacity represents the strength level beyond which the response of the building is strongly nonlinear and is higher than the design strength, due to minimum code requirements, actual strength of materials being higher than the design one (mean values of concrete and steel strength were used in the nonlinear analyses) and, most important of all, due to the presence of masonry infills (this influence is more pronounced in the case of frame systems), whenever such infills are present. The ultimate capacity is related to the maximum strength of the building when the global structural system has reached a full mechanism. It is emphasised that due to the fact that the pushover curves used for the vulnerability assessment are bilinear versions of the actually calculated curves (see Fig. 3), a necessity arising from the fact that bilinear behaviour is considered in reducing the elastic spectrum to an inelastic one (or an equivalent elastic one for effective damping compatible with the energy dissipated by the inelastic system), the ‘ultimate’ capacity generally does not coincide with the actual peak strength recorded during

the analysis. Moreover, the ‘yield’ capacity is not the strength of the building when first yielding of a member occurs. The proper way to ‘bilinearise’ a pushover curve is still a rather controversial issue, in the sense that different methods are more appropriate, depending on the objective of the specific analysis. It is worth recalling here that in the ATC-40 (1996) manual, where the capacity spectrum method is presented in detail, it is recommended to bilinearise the capacity curve with respect to the previously estimated target point, i.e. the bilinearised curve changes during each iteration, which is not a very convenient procedure.

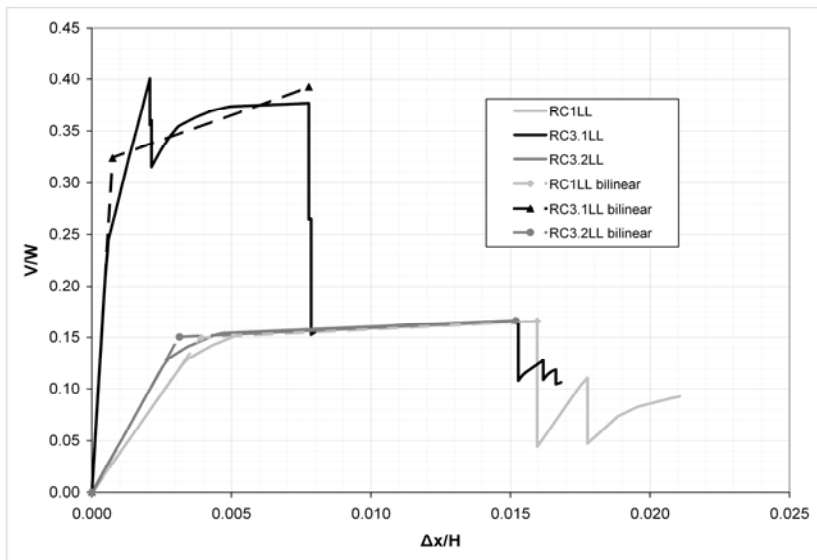


Figure 3. Pushover curves for low-rise R/C frames designed to old codes.

Using standard conversion procedures (e.g. ATC 1996, FEMA-NIBS 2003), pushover curves ( $V/W$  vs.  $\Delta x/H_{tot}$ ) were transformed into capacity curves ( $S_a$  vs.  $S_d$ ). The coordinates of the points describing the pushover and the capacity curves are given for all R/C frame typologies studied in Table 1. It is pointed out that in other commonly used methodologies such as HAZUS (FEMA-NIBS 2003),  $S_{au}$  is defined as the point corresponding to the formation of a full plastic mechanism, whereas in the method proposed herein  $S_{au}$  is defined as the displacement of the building whenever a significant drop in strength occurs (as discussed earlier); at the level of fragility assessment,  $S_{au}$  should be related to the displacement at which the building reaches a certain damage state (e.g. DS4 or DS5, see section 3). The major difference between the strengths of bare (RC1) and regularly infilled (RC3.1) buildings is particularly noted; for N or L buildings the presence of infills more than doubles the ultimate capacity, whereas for H buildings the increase is about 50%. Another important observation is that in dual structures (not included in table 1), which are the most common R/C building type in Greece since the eighties, the presence of infills has a much lesser effect on strength, and the difference between the corresponding three classes (RC4.1, 4.2 and 4.3) are such as to warrant lumping them in one single class (RC4) for vulnerability assessment purposes (Kappos et al. 2006).

Infilled R/C buildings (such as RC3.LL and RC3.2LL in Fig. 3) should be treated with caution: Since reduced spectra (inelastic, or elastic for effective damping ratios higher than 5%) are based on bilinear skeleton curves, it is not feasible (at least at this stage) to introduce multilinear pushover or capacity curves (i.e. including residual strength branches), hence it is suggested to tackle the problem as follows:

- make use of the curves for which parameters are shown in Table 1 as long as the spectral displacement considered remains lower than the given  $S_{du}$ .

- for greater  $S_d$  values, analysis of the regularly infilled building should be repeated using the capacity curve for the corresponding bare one (RC1 or RC4.1); in some cases (particularly for pre-code or low-code buildings) it might be justified to use an  $S_{du}$  value slightly reduced with respect to the bare frame, but this refinement is probably not warranted in the light of all the uncertainties involved.
- for pilotis buildings (RC3.2) it is conservatively suggested to assume that  $S_{du}$  values as reported in Table 1 are the actual ultimate values, except for the High Code case for which the procedure suggested for regularly infilled frames could be used.

Some example curves were shown in figure 3 for R/C frame buildings designed to old codes (L); shown in the figure are (from top to bottom) the cases of infilled, pilotis and bare building, respectively. It is clear from these plots that subsequent to failure of the ground storey infill walls the strength of (fully) infilled frames becomes very close to that of the corresponding bare frame, while its ultimate deformation is somewhat lower. It is noted, though, that a ‘global type’ analysis that cannot fully capture local failure to R/C members due to interaction with infill walls, in principle can not yield a reliable ultimate displacement for the structure; more work is clearly needed in this direction.

Table 1. Capacity curve parameters for frame buildings

Building type	Yield Capacity Point		Ult. Capacity Point	
	$S_{dy}$ (cm)	$S_{ay}$ (g)	$S_{du}$ (cm)	$S_{au}$ (g)
RC1LL	1.15	0.187	5.19	0.207
RC1ML	3.28	0.17	9.39	0.174
RC1HL	4.31	0.125	9.91	0.138
RC1LM	1.14	0.398	7.2	0.409
RC1MM	2.72	0.213	12.58	0.218
RC1HM	6.83	0.238	26.28	0.238
RC1LH	4.45	0.746	50.65	0.746
RC1MH	4.9	0.427	58.23	0.456
RC1HH	13.34	0.245	73.65	0.258
RC3.1LL	0.53	0.432	6.74	0.524
RC3.1ML	1.25	0.277	10.62	0.357
RC3.1HL	3.28	0.206	14.55	0.256
RC3.1LM	0.59	0.49	1.4	0.545
RC3.1MM	1.39	0.274	5.27	0.292
RC3.1HM	2.26	0.266	7.68	0.266
RC3.1LH	0.97	0.975	6.06	1.133
RC3.1MH	1.64	0.538	8.12	0.63
RC3.1HH	4.26	0.34	20.22	0.396
RC3.2LL	0.88	0.201	4.68	0.221
RC3.2ML	2.45	0.205	9.89	0.23
RC3.2HL	3.6	0.195	11.31	0.228
RC3.2LM	0.81	0.369	6.82	0.379
RC3.2MM	1.87	0.203	11.26	0.206
RC3.2HM	2.46	0.257	11.37	0.264
RC3.2LH	3.25	0.777	54.51	0.818

RC3.2MH	3.06	0.473	41.42	0.512
RC3.2HH	5.49	0.337	29.98	0.356

## 2.5 Derivation of fragility curves

One possibility for deriving probabilistic vulnerability (fragility) curves is in terms of macroseismic intensity (I) or PGA; it is recalled herein that as long as a certain empirical (attenuation) relationship between I and PGA is adopted, the two forms of fragility curves (in terms of I or PGA) are exactly equivalent. The assignment of a PGA to the statistical damage database (Penelis et al. 1989) used within the hybrid method was made using the relationship

$$\ln(\text{PGA})=0.74 \cdot I+0.03 \quad (2)$$

which is one of the most recent ones proposed for Greece (Koliopoulos et al. 1998) and is based on statistical processing of a large number of Greek strong ground motion records; it is calibrated for intensities less than 9, and should not be used for  $I > 9$ .

Assuming a lognormal distribution (common assumption in seismic fragility studies), the conditional probability of being in or exceeding, a particular damage state  $ds_i$ , given the peak ground acceleration (PGA) is defined by the relationship

$$P[ds \geq ds_i / \text{PGA}] = \Phi \left[ \frac{1}{\beta_{ds_i}} \ln \left( \frac{\text{PGA}}{\overline{\text{PGA}}_{ds_i}} \right) \right] \quad (3)$$

where:

$\overline{\text{PGA}}_{ds_i}$  is the median value of peak ground acceleration at which the building reaches the threshold of damage state,  $ds_i$ , see Table 2.

$\beta_{ds_i}$  is the standard deviation of the natural logarithm of peak ground acceleration for damage state,  $ds_i$ , and

$\Phi$  is the standard normal cumulative distribution function.

Table 2. Damage grading and loss indices (% of replacement cost) for R/C and URM buildings

Damage State	Damage state label	Range of loss index -R/C	Central index (%)
DS0	None	0	0
DS1	Slight	0-1	0.5
DS2	Moderate	1-10	5
DS3	Substantial to heavy	10-30	20
DS4	Very heavy	30-60	45
DS5	Collapse	60-100	80

Each fragility curve is defined by a median value of peak ground acceleration that corresponds to the threshold of that damage state and by the variability associated with that damage state; these two quantities are derived as described in the following.

Median values for each damage state in the fragility curves were estimated for each of the 54 types of building systems analysed. The starting point for estimating these values is the plot of the damage index (calculated from inelastic time history analysis as described in section 2.3) as a function of the earthquake intensity (PGA), for which the name primary vulnerability curve is proposed; some plots of this type are given in Fig. 4 and they refer to buildings with frame system designed to moderate codes (see section 2.1). Several trends can be identified in the figure, for instance that the least vulnerable building is the fully infilled one, with the exception of very low PGA values, for which the loss is higher than in the other two types; this is mostly due to damage in the masonry infills, which is accounted for in the loss model used (Kappos et al. 1998b).

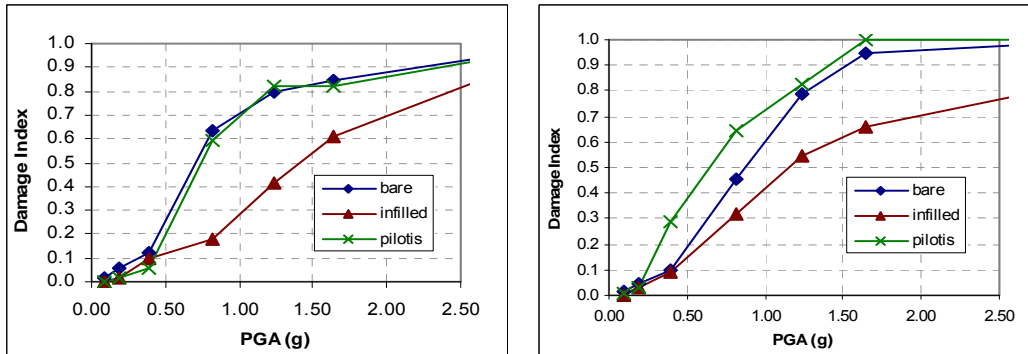


Figure 4. Evolution of economic damage (loss) index for medium-rise (left) and high-rise (right) buildings with R/C frame system designed to 'moderate' codes.

Median values (for equation 3) are then estimated based on the hybrid approach, which combines inelastic dynamic analysis and the database of the Thessaloniki earthquake of 1978 (Penelis et al., 1989), corresponding to an intensity  $I=6.5$ , to which a peak ground acceleration of  $0.13g$  corresponds, according to the adopted  $I - PGA$  relationship (equation 2); it is noted that this PGA practically coincides with the one of the only record available from the 1978 earthquake in Thessaloniki. From the database of the Thessaloniki earthquake, the damage index, defined here as the ratio  $L$  of repair cost to replacement cost (i.e. as a direct loss index), corresponding to this PGA is found for each building (a total of 5700 R/C buildings are included in the database). The Thessaloniki database is described in a number of previous publications (Penelis et al., 1989; Kappos et al. 1998b); a brief reference to this as well as to some other Greek databases is made in section 3.2 of this chapter (focussing on masonry buildings).

Having established analytically the loss index  $L$ , the final value to be used for each PGA in the fragility analysis depends on whether an empirical value is available for the PGA or not, i.e. (see also Kappos & Panagopoulos 2009):

(i) if the 'actual' (empirical) loss value at a point  $i$  ( $PGA=PGA_i$ ),  $L_{act,i}$  is available in the database, the final value to be used is

$$L_{fin,i} = w_1 L_{act,i} + w_2 L_{anl,i} \quad (w_1 + w_2 = 1) \quad (4)$$

where  $L_{anl,i}$  is the analytically calculated loss value (cf. Fig. 4) for that  $PGA_i$  and  $w_1$ ,  $w_2$  are weighting factors that depend on the reliability of the empirical data available at that intensity. If  $L_{act,i}$  is based on more than about 60 buildings,  $w_1$  equal to about 1 is recommended, if it is based on 6 buildings or less,  $w_1$  should be taken as zero (or nearly so).

(ii) if the 'actual' (empirical) loss value at a point  $j$  ( $PGA_j$ ),  $L_{act,j}$  is not available in the database, the final value to be used is

$$L_{fin,j} = \frac{1}{2} (\lambda_i + \lambda_k) L_{anl,j} \quad (5a)$$

where  $\lambda_i, \lambda_k$  are the ratios  $L_{fin}/L_{anl}$  at points  $i, k$ , hence

$$\lambda_i = w_1(L_{act,i}/L_{anl,i}) + w_2 \quad (5b)$$

and  $PGA_i < PGA_j < PGA_k$ . Clearly, this is an interpolation scheme that aims to account (in a feasible way) for the strongly nonlinear relationship between intensity and damage. In the common case that  $L_{act}$  is available at one or very few points the scheme should be properly adapted by the analyst.

It is worth noting that the ratios  $L_{act}/L_{anl}$  calculated for the Thessaloniki 1978 data were reasonably close to 1.0 when the entire building stock was considered, but discrepancies for some individual building classes did exist (Kappos et al., 1998b). In this way it is possible to establish a relationship between damage index and PGA for each building type (similar to the one shown in Fig. 4, but now accounting for the empirical data as well), and consequently to assign a median value of PGA to each damage state. Table 2 provides the best estimate values for the loss index ranges associated with each damage state, derived from previous experience with R/C structures (Kappos et al. 2006).

Lognormal standard deviation values ( $\beta$ ) describe the total variability associated with each fragility curve. Three primary sources contribute to the total variability for any given damage state (FEMA-NIBS, 2003), namely the variability associated with the discrete threshold of each damage state which is defined using damage indices (in the present study this variability includes also the uncertainty in the models correlating structural damage indices to *loss*, i.e. the ratio of repair cost to replacement cost, see also Kappos 2001), the variability associated with the capacity of each structural type, and finally the variability of the demand imposed on the structure by the earthquake ground motion. The uncertainty in the *definition of damage state*, for all building types and all damage states, was assumed to be  $\beta=0.4$  (FEMA-NIBS, 2003), the variability of the *capacity* for low code buildings is assumed to be  $\beta=0.3$  and for high code  $\beta=0.25$  (FEMA-NIBS), while the last source of uncertainty, associated with *seismic demand*, is taken into consideration through a convolution procedure, i.e. by calculating the variability in the final results of inelastic dynamic analyses carried out for a total of 16 motions at each level of PGA considered.

The last part of fragility analysis was carried out using in-house developed software (HyFragC), which permitted quick exploration of alternative approaches (sensitivity analysis). Parameters of the cumulative normal distribution functions derived for two specific classes (R/C frame structures designed to ‘low-code’ and ‘moderate code’) are given in Table 3; similar results are available for all other cases studied. Example fragility curves constructed are given in Figure 5.

Referring first to Table 3, it is noted that beta-values are given as constant for each building type; this constant value (estimated to be between about 0.6 and 0.7) is the average of the 5 values of beta corresponding to each of the 5 damage states. This was done on purpose, because if the (generally) different variability associated with each damage state (calculated from the results of time-history analysis) is taken, unrealistic fragility curves (for instance, intersecting) result in cases where median values are closely spaced (e.g. see Fig. 5-top, DS3 and DS4).

Table 3. Fragility curve parameters for buildings with R/C frame system, designed to Low and Moderate code.

Building type	DS1	DS2	DS3	DS4	DS5	$\beta$
RC1LL	0.001	0.012	0.096	0.157	0.219	0.733
RC3.1LL	0.021	0.101	0.201	0.257	0.343	0.733
RC3.2LL	0.005	0.049	0.116	0.181	0.230	0.733
RC1ML	0.001	0.013	0.095	0.136	0.192	0.651
RC3.1ML	0.005	0.055	0.190	0.216	0.254	0.651
RC3.2ML	0.000	0.004	0.042	0.099	0.136	0.651
RC1HL	0.006	0.061	0.149	0.276	0.545	0.629
RC3.1HL	0.013	0.097	0.210	0.296	0.548	0.629
RC3.2HL	0.044	0.101	0.209	0.353	0.673	0.629
RC1LM	0.002	0.023	0.148	0.413	0.639	0.733
RC3.1LM	0.090	0.123	0.298	0.730	1.391	0.733
RC3.2LM	0.005	0.051	0.215	0.497	0.748	0.733
RC1MM	0.001	0.014	0.115	0.297	0.844	0.651
RC3.1MM	0.008	0.078	0.201	0.422	0.853	0.651
RC3.2MM	0.001	0.011	0.116	0.476	0.795	0.651
RC1HM	0.006	0.056	0.363	1.471	2.724	0.629
RC3.1HM	0.017	0.109	0.419	0.923	3.471	0.629
RC3.2HM	0.015	0.110	0.525	1.103	2.370	0.629

Different sets of fragility curves are plotted in Fig. 5 (full and dotted lines), the difference lying in the way empirical data were introduced (cf.  $w_1$ ,  $w_2$  factors in equation 4). The effect on the resulting curves appears to be rather significant, particularly for the higher damage states. Also, as anticipated, the effect of seismic design is significant; buildings designed to only a ‘moderate’ seismic code are seen to be substantially less vulnerable than buildings designed to ‘low’ code, pointing to the importance of using some basic seismic design rules (like basic capacity design and ductility), even if these rules are not in compliance with modern code provisions.

It is worth pointing out here that the way fragility curves were developed here (for all common building types) using the hybrid approach at the stage of producing damage grade vs. earthquake intensity relationships (see Fig. 4) is different from other procedures in the literature, which are based either on fitting of curves directly to empirical data (e.g. Spence et al. 1992) or on expert judgement (e.g. ATC 1985). It is also different from the empirical approach used by other researchers within the RISK-UE project (Lagomarsino & Giovinazzi 2006). Finally, it is different (although the basic idea of the hybrid approach is retained) from the procedure used by the AUTH group for defining fragility curves for URM buildings (see section 3).

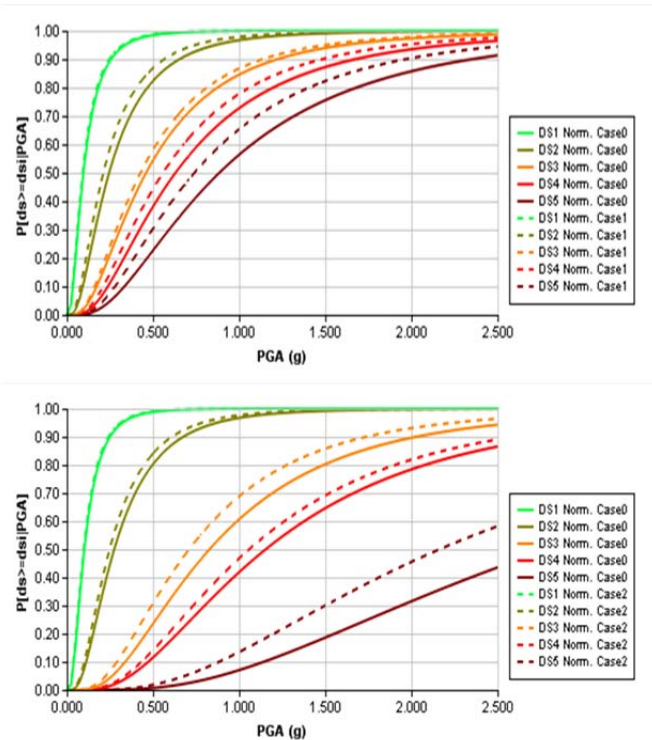


Figure 5. Hybrid vulnerability curves for R/C dual structures, derived from different interpretation of empirical data: low-rise, low-code buildings with infills (top); medium-rise, moderate code buildings with pilotis (bottom).

## 2.6 Fragility curves in terms of $S_d$

The aforementioned fragility curves in terms of PGA were also used to derive additional curves, this time in terms of  $S_d$ , necessary for fragility assessment using the HAZUS approach (FEMA-NIBS 2003). The procedure adopted was to transform the median PGA values to corresponding median  $S_d$  values, using an appropriate spectrum and either the fundamental period of the ‘prototype’ building, assuming that the equal displacement rule applies, or using the capacity spectrum approach (for short period buildings). It is noted that the convenient equal displacement approximation (inelastic displacement demand approximately equal to elastic demand) is a valid assumption for medium-rise and high-rise buildings, but usually a crude one for low-rise buildings. Effective periods are involved, corresponding to the structure’s characteristics at yield, hence periods are longer than the elastic ones, e.g. considering the 2-storey frame building,  $T_{ef} \approx 0.5s$  for bare frames, but  $T_{ef} \approx 0.2s$  for the fully infilled frames. For the present application of the methodology it was decided to use the mean spectrum of the microzonation study of Thessaloniki (Anastasiadis et al., 2001) since the derived  $S_d$ -based fragility curves were primarily intended to be used for the Thessaloniki risk scenario (Pitilakis et al. 2004). Clearly other options are also available, the most conservative one being to use the seismic code design spectrum, which has been found to overestimate seismic actions (particularly displacements) for medium and long period structures (Athanasiadou et al. 2007, 2011).

Two examples of  $S_d$ -based fragility curves are given in Figure 6 (4-storey infilled frames, designed to ‘low’ or ‘high’ codes). A more detailed discussion of the impact the type of fragility curve used for a vulnerability assessment study has on its results (loss scenario) is given by the author and his co-workers in Pitilakis et al. (2004), wherein the damage and loss scenario for Thessaloniki, developed using both approaches, is presented.

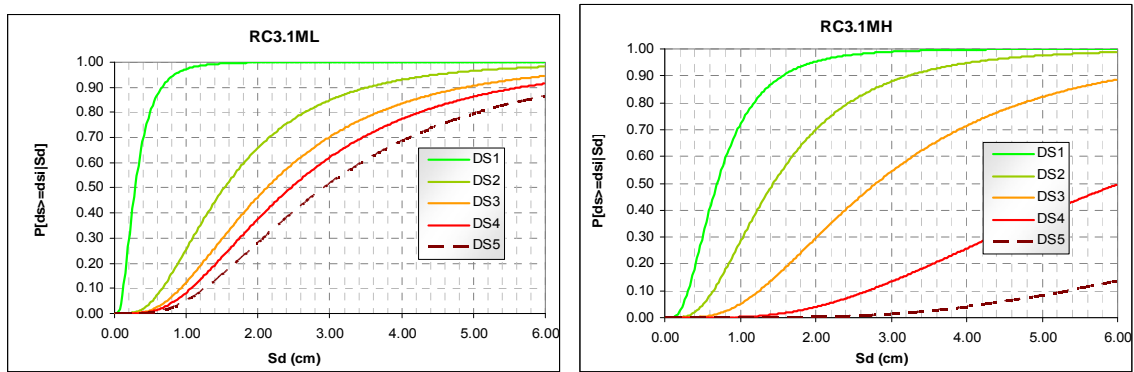


Figure 6.  $S_d$ -based fragility curves for medium-rise infilled R/C frames, low-code (left) and high-code design.

### 3 Vulnerability assessment of URM buildings

#### 3.1 Overview of the methodology adopted

For URM buildings, apart from the Thessaloniki 1978 earthquake data (used for R/C structures, see section 2), the database from the Aegion 1995 event (Fardis et al. 1999) was also utilised. The first step for the utilisation of these two databases was the assignment of an appropriate intensity (or corresponding PGA) for the area they refer to. A value of 7 was adopted for Thessaloniki and a value of 8 for Aegion. These databases were used for the simple, purely statistical, procedure described in section 3.2, and were extrapolated to lower and higher events using nonlinear analysis in the hybrid approach described in sections 3.3 and 3.4.

#### 3.2 Purely empirical approach

A purely empirical approach (similar to that used by other researchers, e.g. Spence et al. 1992, Lagomarsino & Giovinazzi 2006), was first adopted by the authors for deriving fragility curves in terms of intensity for URM buildings. For these buildings statistical data were available for more intensities, hence it was conceptually feasible to adopt a purely empirical approach, as opposed to the hybrid one used for R/C buildings (section 2.5); the latter was also used for deriving fragility curves for URM buildings (section 3.4). The empirical procedure initially adopted was quite straightforward and consisted in curve fitting the available damage data from the aforementioned events. A more refined procedure based on the vulnerability index method (Lagomarsino & Giovinazzi 2006) was also used.

The Thessaloniki database (Penelis et al. 1989) consists of a record of the centre of the city of Thessaloniki with randomly selected buildings with a density of 1:2 (i.e. 50% of total building stock within the selected area was recorded) with all the relevant information included, such as year of construction, material, number of storeys, first level post-earthquake damage classification (green-yellow-red tag), and (importantly) cost of repair of earthquake damage. The database includes a total of 5740 buildings, 1780 of which (31%) are unreinforced masonry ones, and most of the remaining buildings are reinforced concrete ones.

The database does not include specific information regarding the type of masonry (stone or brick), therefore the assumption that all URM buildings constructed before 1940 were stone masonry and all the rest brick masonry, was adopted, based on historical evidence on types of masonry construction in Greece (Kappos et al. 2006). Details of the processing of the database are given in Penelis et al. (2002), where the reasons are discussed why economic

damage indices (ratio of repair cost to replacement cost) and post-earthquake tagging of buildings ('green'-'yellow'-'red') had to be combined in interpreting the Thessaloniki data. Table 4 summarises the distribution of economic damage (5 damage states were considered, in addition to zero-damage, see Table 2) in the main categories of URM buildings, i.e. *stone* masonry (Stone1-3 is for all buildings, which had from one to three storeys, Stone1 and Stone2 refer to single-storey and two-storey buildings, respectively), and *brick* masonry (symbols analogous to those used for Stone).

Table 4. Damage matrix (% of buildings in each DS) for Thessaloniki 1978 data, based on economic damage index

Damage State	Stone 1-3	Stone1	Stone2	Brick 1-3	Brick1	Brick2
DS0	60.6	64.4	52.3	77.6	76.0	78.9
DS1	13.8	12.9	14.1	9.2	9.2	10.0
DS2	13.7	12.9	14.1	9.2	9.3	10.0
DS3	5.5	4.9	8.4	3.6	5.0	1.1
DS4	4.3	3.8	6.5	0.2	0.2	0.0
DS5	1.9	1.2	4.6	0.2	0.3	0.0
Mean damage factor	0.75	0.69	0.93	0.39	0.44	0.33

The Aegion database (Fardis et al. 1999) includes all buildings within the centre of Aegion, among them the vast majority of the damaged R/C and URM buildings. The sample consists of 2014 buildings, 857 of which (42.5%) are unreinforced masonry buildings. The database was set up on the basis of four non-zero damage levels (DS0 to DS4); to convert it to the 5-level classification scheme the last level (DS4) has been divided into two (DS4 and DS5) at a proportion of 70 and 30%, respectively, in general conformity with the corresponding Thessaloniki data. Characterization of each building's damage state was performed by visual inspections carried out by the research team of the University of Patras. This approach eliminates the risk of overestimating damage that is present when using the cost of repair criterion, but on the other hand is more subjective, heavily relying on experience and judgment during the visual inspection. Damage matrices derived on the basis of Aegion data for the two categories (brick and stone) that are also used in the Thessaloniki database are given in Penelis et al. (2002), who also made some limited use of a third database, including data from the 1993 Pyrgos earthquake.

Empirical curves were first derived using the aforementioned databases and an exponential type of statistical model and they are reported in Kappos et al (2006); albeit useful, they are not deemed as sufficiently reliable, since data for only two intensities were available. It should be noted that the empirical approach, simplistic it may seem, requires sophisticated statistical filters and correlations for different databases derived for different parts of a country and by different research groups, to ensure compatibility between them and remove outliers, such as damage data for a specific building type and intensity 8 being lower than that for an intensity 7 event. In view of the limited data available, additional statistical data from Italian events were also used in order to calibrate the recorded damage data in the aforementioned databases. A second interpretation of the available data using the vulnerability index approach (Lagomarsino & Giovinazzi 2006), re-assigning the intensities of Thessaloniki and Aegion to 6.5 and 7, respectively (based on comparisons with the Italian

data), and finally using beta distributions for the fragility curves, resulted in the sets of curves shown in Figure 7 (Penelis et al. 2002); these curves are drawn in terms of four (rather than five) damage states. Note that no differentiation on the basis of building height is made in these sets of curves.

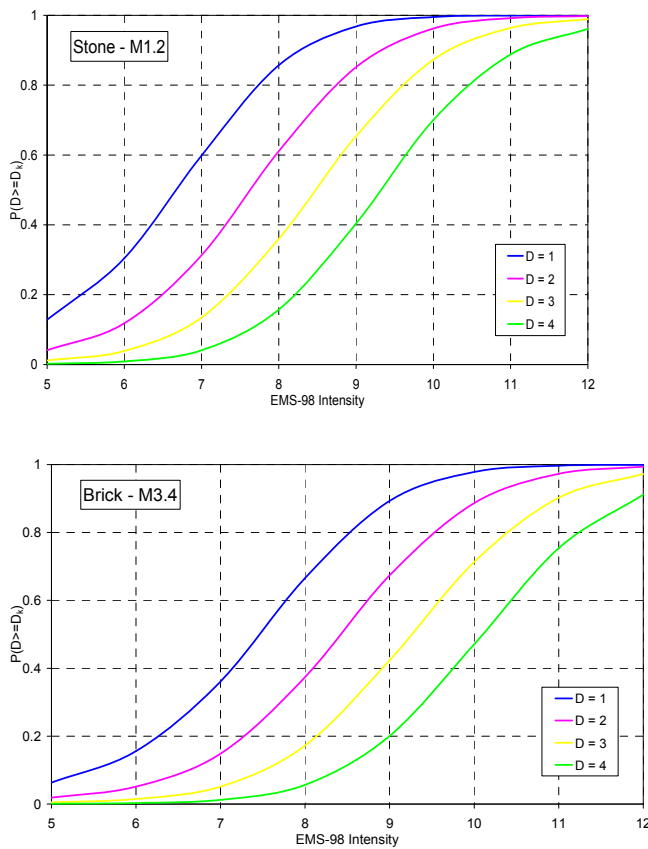


Figure 7. Empirical fragility curves (beta distributions) for stone masonry (top) and brick masonry buildings.

### 3.3 Nonlinear analysis and capacity curves

It is well known that the nonlinear response of unreinforced masonry (URM) buildings is not easy to model, mainly because the frame element (beam-column) commonly used in the case of R/C buildings is generally not amenable to modelling URM buildings. The difficulties are increased in the case of dynamic analysis where the inertia forces should not be concentrated at the diaphragm levels (which is the rule for R/C buildings). Therefore, for the study reported here, an alternative procedure was adopted for the evaluation of the economic loss in URM buildings, based on the use of capacity curves (estimated using pushover analysis) and fragility curves, wherein the probability of exceeding a certain damage state is expressed in terms of spectral displacement (rather than Intensity or PGA).

The curves presented herein refer mainly to simple stone masonry and brick masonry buildings, with sufficiently stiff floors to provide diaphragm action, such as reinforced concrete floor slabs or vaulted floors, which are by far the most common URM building types in Thessaloniki, as well as in the rest of Greek cities (see also Penelis et al. 2002). These two main categories are further subdivided into single-storey, two-storey and three-storey buildings. More specifically, the generic structure considered followed the layout shown in figure 8 and was used for one, two, and three storey URM buildings. This layout corresponds

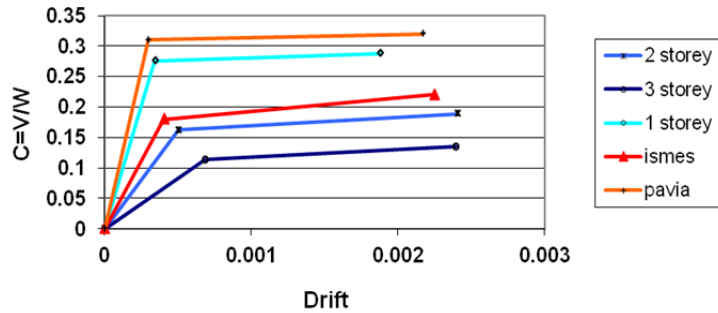


Figure 9. Pushover curves grouped per number of storeys category, and experimental curves from the literature (Pavia and Ismes tests on two-storey buildings).

Table 5. Capacity curve parameters for URM buildings

	BTM type	Yield point		Ultimate point	
		$S_{dy}$ (cm)	$S_{ay}$ (g)	$S_{du}$ (cm)	$S_{au}$ (cm)
material B	M1.2-1st	0.136	0.320	0.563	0.328
	M1.2-2st	0.374	0.189	1.633	0.214
	M1.2-3st	0.774	0.135	2.335	0.158
material A	M3.4-1st	0.075	0.231	0.588	0.248
	M3.4-2st	0.250	0.135	1.347	0.164
	M3.4-3st	0.506	0.092	2.132	0.111
	MEAN	0.352	0.184	1.433	0.204

Using the same procedure as for R/C structures (section 2.4), capacity curves have been derived for one, two, and three storey URM buildings, belonging to the types M1.2 ('simple stone' URM buildings) and M3.4 (URM buildings with R/C floors). The corresponding parameters for these curves are given in Table 5. According to the RISK-UE building typology matrix (Lagomarsino & Giovinazzi 2006), single-storey and two-storey buildings of the same material (stone or brick) should be grouped into a single category (M1.2L and M3.4L), which does not seem to be a sound choice, given the distinctly different properties of the corresponding capacity curves shown in Table 5.

### 3.4 Hybrid fragility curves

The hybrid methodology described in previous sections was used to calculate vulnerability (fragility) curves for URM buildings in terms of spectral displacement. When appropriate capacity curves are available (as is the case here), the straightforward procedure (used in HAZUS) to derive fragility curves consists in defining damage states in terms of structure displacements (typically top storey drift) and transforming these into displacements of the equivalent SDOF system, i.e. spectral displacements; these are then used as the mean values of the lognormal distribution defined for each damage state. The corresponding variabilities ( $\beta$  values) can be estimated in a way similar to that described for R/C structures (section 2.5). Instead of using semi-empirical interstorey drift values (the HAZUS approach), the AUTH group (Kappos 2001, Kappos et al. 2006) has suggested expressing the damage state thresholds in terms of the basic parameters of the capacity curve (yield displacement and ultimate displacement, both referring to a bilinearised capacity curve); this proposal is shown

in Table 6. It should be clear that, depending on the height of the building and the failure mechanism,  $S_{dy}$  and  $S_{du}$  values vary for each building type.

Table 6. Damage states in terms of displacements, and associated loss indices (%), for URM buildings

Damage State	Damage state label	Spectral displacement	Range of loss index
DS0	None	$<0.7S_{dy}$	0
DS1	Slight	$0.7S_{dy} \leq S_d < S_{dy}$	0-4
DS2	Moderate	$S_{dy} \leq S_d < 2S_{dy}$	4-20
DS3	Substantial to heavy	$2S_{dy} \leq S_d < 0.7S_{du}$	20-50
DS4	Very heavy	$0.7S_{du} \leq S_d < S_{du}$	50-100
DS5	Collapse	$>S_{du}$	

Although straightforward, the aforementioned procedure cannot be directly integrated within the hybrid approach. For the latter to be materialised, one possible way is to define damage states in terms of the loss index, already used in the case of R/C structures. Four damage states (plus the no-damage state) are proposed for URM buildings, defined according to the loss index (L) shown in Table 6; note that the range of L for each state is different from that used for R/C buildings (Table 2). To correlate these damage states to an analytical expression of damage, the loss index was expressed as a function of yield and ultimate displacement of each building, as shown in figure 10; this model is based on the definitions of damage in terms of spectral displacement shown in the third column of Table 6, but recognising that for  $\Delta > 0.9\Delta_u$ , a URM building should be replaced (L=100%) rather than repaired.

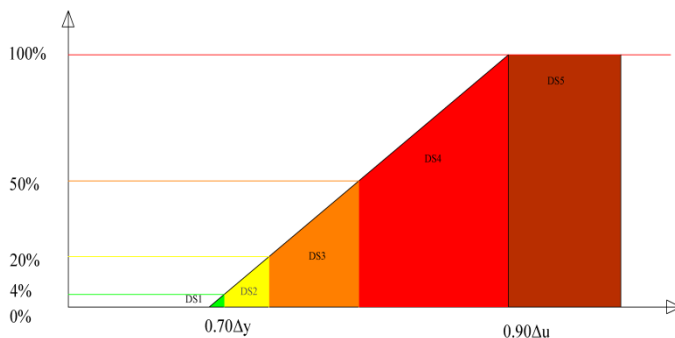


Figure 10. Economic loss index in URM buildings, as a function of roof displacement.

Fragility curves were then calculated by scaling down the Thessaloniki database and scaling up the Aegion database, with scaling factors derived using the model of fig. 10. To derive the scaling factors, spectral displacements were associated with each of those two events (Thessaloniki and Aegion), calculated from the recorded accelerograms in each site and the corresponding pushover curves (see fig. 9) for one, two, and three storey URM buildings, using the capacity spectrum procedure (FEMA-NIBS 2003). It is noted that the relationship between scaling factors for actual loss values (cost of repair of each building in the database to corresponding replacement cost) in the Thessaloniki and Aegion databases is not constant for all building types, since the spectral displacement associated with each building type is generally different. Moreover, the  $S_d$ -based procedure is sensitive to the type

of ‘representative’ response spectra selected for each earthquake intensity (for instance, the recorded accelerogram used in each city is not necessarily representative of the earthquake shaking in the entire area studied). The issue of ground motion dependence of fragility curves is further elaborated in section 4.

Using the hybrid procedure, damage histograms were constructed for the URM building classes of interest; among these histograms, the ones corresponding to the  $S_d$  values assigned to the Thessaloniki and Aegion earthquakes consisted of actual loss values, while the rest were derived by the scaling procedure described previously. To these histograms were fitted lognormal cumulative distributions of the type:

$$P[ds \geq ds_i | S_d] = \Phi \left[ \frac{1}{\beta_{ds}} \ln \left( \frac{S_d}{S_{d,ds}} \right) \right] \tag{6}$$

which is similar to equation (3), only that  $S_d$  is used instead of PGA.

Figure 11 shows two sets of vulnerability curves plotted against the actual data from the databases; as expected, for the same height, stone masonry buildings show higher vulnerability than brick masonry buildings.

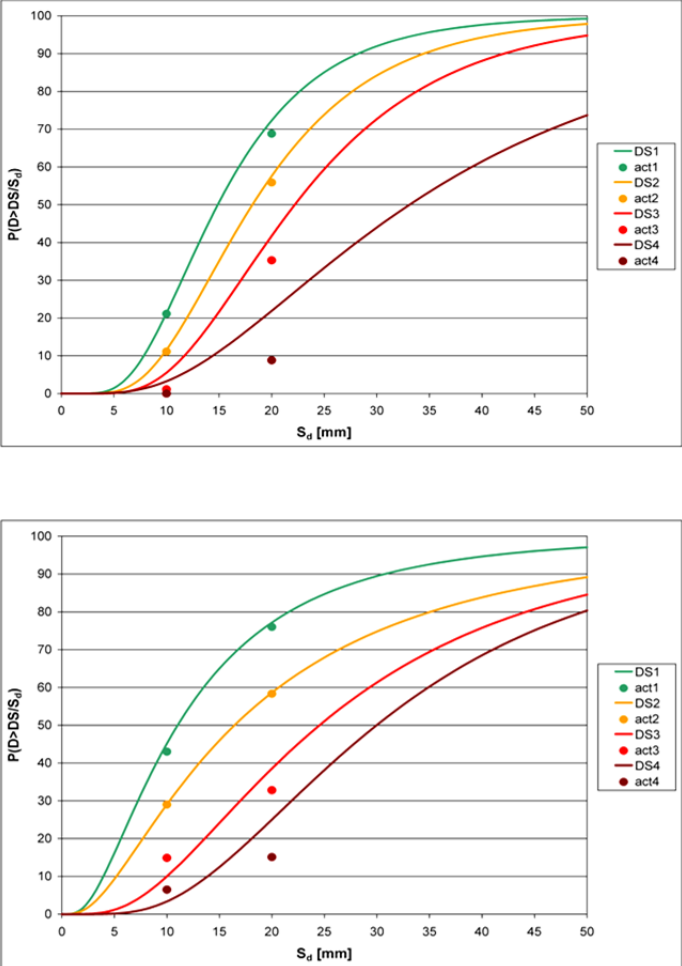


Figure 11. Hybrid vulnerability curves for masonry buildings: 2-storey brick masonry (top) and 2-storey stone masonry (bottom).

## 4 Region-specific fragility curves

A key feature of fragility curves derived on the basis of a specific set of ground motions is that, unlike the purely analytical HAZUS-type fragility curves, which are independent of the ground motion characteristics since they are derived in terms of normalised displacement values (interstorey drifts), the motion-specific curves (e.g. derived in terms of PGA as shown in Fig. 6) are dependent on the spectral characteristics of the accelerograms used. Hence, a critical step in applying such curves to a specific study is to make them region-specific, i.e. dependent on the characteristics of the representative ground motions in the cities studied, which can be quite different from those used for deriving the PGA-based curves (and also  $S_d$ -based hybrid curves that involve assuming a specific spectral shape, see section 3.4). To this purpose, the simple procedure proposed by Kappos et al. (2010) can be implemented, wherein a further processing of the ‘generic’ fragility curves is carried out by scaling their damage state thresholds to match the spectrum intensity of the representative pseudo-velocity spectrum in each city, as described in the following, with reference to a specific case-study the Grevena (Greece) and Düzce (Turkey) microzonation studies.

The mean acceleration spectrum of the 16 records of Fig. 2, normalised to a PGA of 1.0g, is illustrated in Fig. 12, together with the mean spectra derived from the Grevena and Düzce microzonation studies (Pitilakis et al. 2010) and the Greek and Turkish Code design spectra for soil types that are typical for the two cities. In this figure it is clear that the spectral accelerations predicted by the Grevena (microzonation-derived) mean spectrum are significantly lower than those corresponding to the mean spectrum that was used for the derivation of the fragility curves, for almost the entire period range (i.e. up to about 2.0sec). This observation leads to the conclusion that the fragility curves derived using the aforementioned procedure provide a rather conservative estimate of the vulnerability of the specific building stock. The scaling was carried out by modifying the median values of the hybrid fragility curves using a uniform correction factor  $c$ , calculated from the ratio of the area enclosed under each pseudo-velocity spectrum ( $S_{pv}$ ) for a period range from 0.1 to 2.0 sec as follows:

$$c = E_{hfc} / E_{micr} \quad (7)$$

where  $E_{hfc}$  and  $E_{micr}$  denote the area under the mean pseudo-velocity spectrum of the records used for the derivation of the hybrid fragility curves and the microzonation study respectively (herein referring to the Grevena case). Using Eq. 7, a value of  $c$  equal to 1.38 was calculated and was then used for the correction of all damage state medians in the R/C fragility curves, regardless of the building class they referred to.

Unlike the Grevena case, the mean spectrum of the microzonation study of Düzce (Fig. 12-right) lies very closely to the mean spectrum of the records used for the derivation of R/C buildings fragility curves, at least for the period range 0.1 to 0.7sec, which is essentially the period range for practically the entire (low-rise) building stock of the old city. As a result, the value of the correction factor  $c$  defined in Eq. (7) was taken equal to unity.

This approach is quite general but very convenient for deriving region- or site-specific analytical fragility curves for a building stock in a specific area (regardless of whether the appropriate ‘target’ spectrum is defined from a microzonation study or a seismic code). Alternatively, a more refined (and more complex) approach can be used involving structural type-dependent  $c$  factors which can be estimated within a period range close to the fundamental period  $T_0$  of each typical building class.

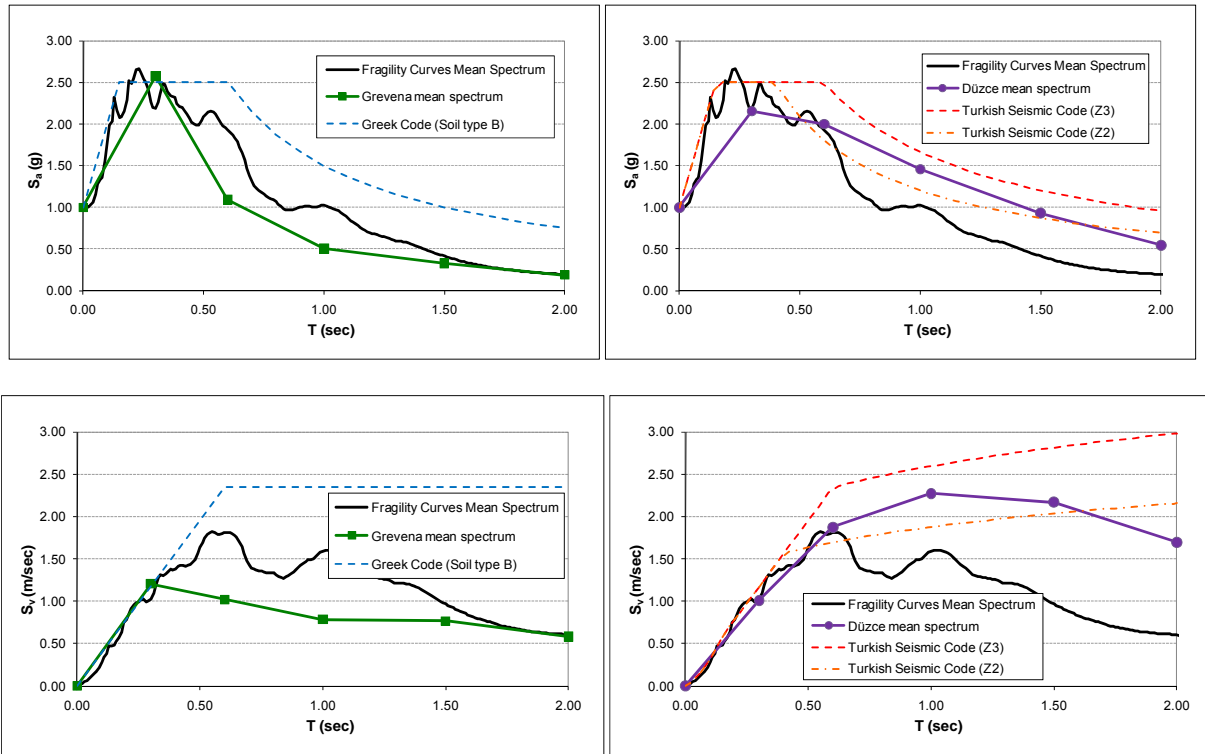


Figure 12. Comparison of the Grevena (left) and Düzce (right) microzonation study mean spectra in terms of acceleration  $S_a$  (top) and velocity  $S_v$  (bottom) with the design spectra of the Greek and Turkish seismic codes and the mean spectrum of the records used for the derivation of fragility curves.

## 5 Development of earthquake scenarios

Two types of scenarios can be developed using the analytical tools presented in the previous sections. In its most rudimentary form the earthquake scenario would simply be an assumption of a uniform intensity for the area studied. An example of such a scenario, concerning the municipality of Thessaloniki (Pitilakis et al. 2004), subjected to a uniform intensity  $I=9$  is shown in Fig. 13. The damage levels were estimated using the PGA-based fragility curves developed for each building type as described in the previous sections; intensity and PGA were correlated using appropriate empirical relationships derived for Greece (Koliopoulos et al. 1998), and the index plotted is a weighted one,  $\Sigma(MDF_i \cdot V_i) / V_{tot}$ , where volume  $V_i$  of each building type is used to weigh the mean damage factor  $MDF_i$  (central index in Table 2) for this type. Such maps give a good picture of the most vulnerable parts of the city, regardless of the specifics of the scenario earthquake (and local amplifications due to particular site conditions), and they are a useful tool in emergency planning, keeping in mind that even an 'accurate' scenario earthquake is just one possible description of the seismic risk in the considered area (i.e. vulnerable buildings not heavily struck by a specific scenario earthquake, might be heavily damaged by a different scenario earthquake not considered due to lack of time and/or lack of data at the time of the study).

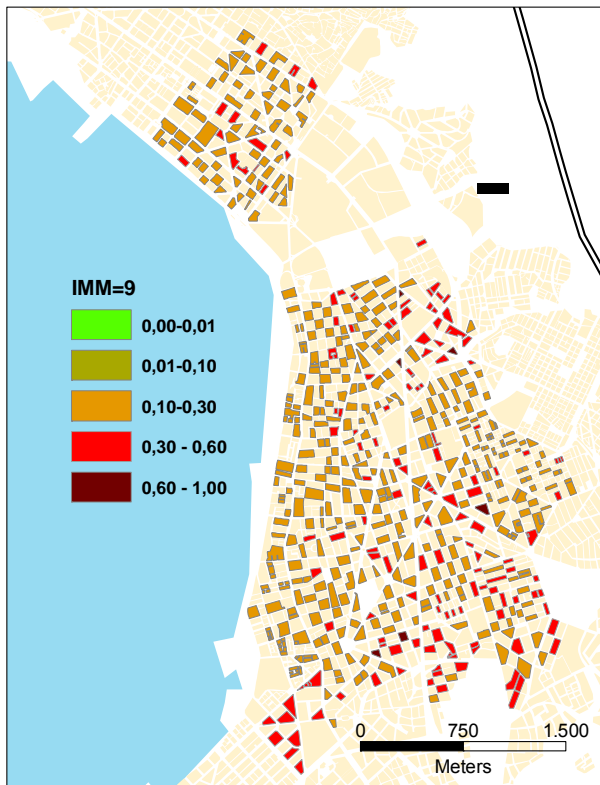


Fig. 13 Expected damage distribution for uniform intensity ( $I_{MM}=9$ ) in the studied area).

A more refined approach is to consider a particular earthquake scenario in terms of PGA distribution (resulting from a scenario earthquake with given location and magnitude) in each 'cell' of the studied area, taking into account ground conditions in each cell; such a PGA distribution scenario for Thessaloniki is reported in Pitilakis et al. (2004) and was used for estimating losses using the fragility curves of sections 2 and 3. The map of Fig. 14 shows the number of buildings suffering damage states DS0 to DS5 in each building block of the studied area, based on the PGA in each building block and the corresponding fragility curves for each building type (R/C or URM). After calculating the discrete probabilities of each damage state (from the fragility curve) for each building type present in a block, the number of buildings suffering each damage state is calculated accordingly; for example, if in a block there are 4 buildings of a particular typology, and the discrete probabilities (derived by subtracting the values determined from the intersection points of the fragility curves and the vertical line corresponding to the given PGA) for DS0 to DS5 are, say, 6, 17, 53, 21, 2, and 1 (%), respectively, two buildings will suffer DS2, one will suffer DS3 and one DS1 (no buildings in the DS0, DS4 and DS5 categories).

It is pointed out that the above is only one of the possible ways of estimating the number of buildings suffering each damage state; it is the most reasonable one (to the author's opinion), but its potential drawback is that in (hypothetical) cases of very uniform distribution of PGA (or any other measure of earthquake intensity) in the studied area, damage states associated with very low probability (e.g. DS4 and DS5 in the previous example) might never appear on the map of DS distribution. As seen in Fig. 14, a non-zero number of buildings exists for all damage states, including even DS5 (collapse), for the considered scenario. Note also that the problem is overcome when units larger than the building block are used in developing the scenario (e.g. neighbourhoods or census tracks), but, of course, such coarser resolutions suffer from other drawbacks, e.g. it is not possible to estimate road closures etc.

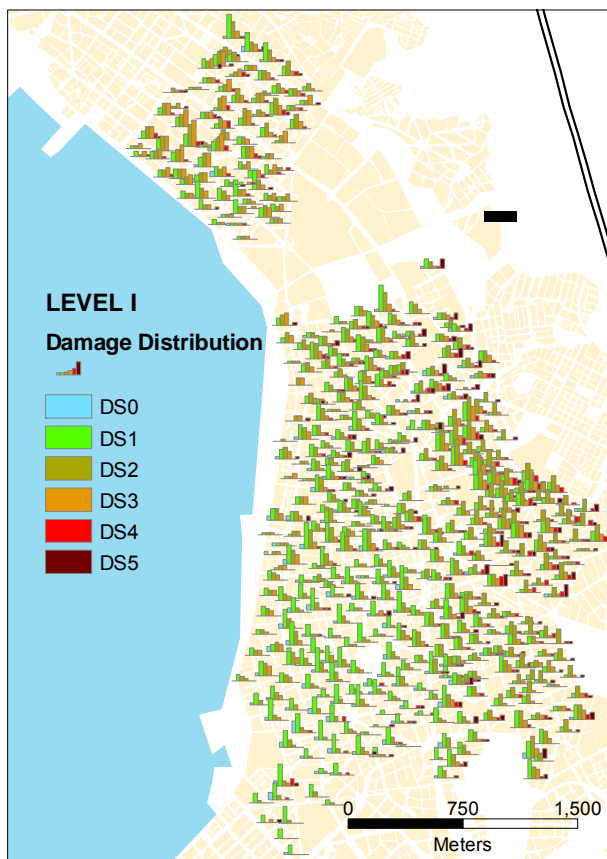


Fig. 14 Number of buildings suffering damage states DS0 to DS5 in each building block (scenario earthquake).

A picture of the expected distribution of post-earthquake tagging of buildings using the familiar Green, Yellow, and Red tag scheme is desirable for earthquake planning purposes. The correspondence between tag colour and DS was assumed as follows:

- Green: DS0 & DS1
- Yellow: DS2 & DS3
- Red: DS4 & DS5

Based on experience from past earthquakes it might well be argued that at least part of DS3 could go to the red tag category. The buildings in each tag category are shown in Figure 15; it is noted that the city is rather vulnerable to the considered earthquake, as about 10% of the buildings will suffer very heavy damage or collapse; this is clearly a far more severe situation than in the 1978 earthquake when there was only one collapse of multistorey R/C building (and at that time all R/C buildings were ‘low-code’ or ‘pre-code’ ones) and heavy damage was observed mainly in masonry buildings.

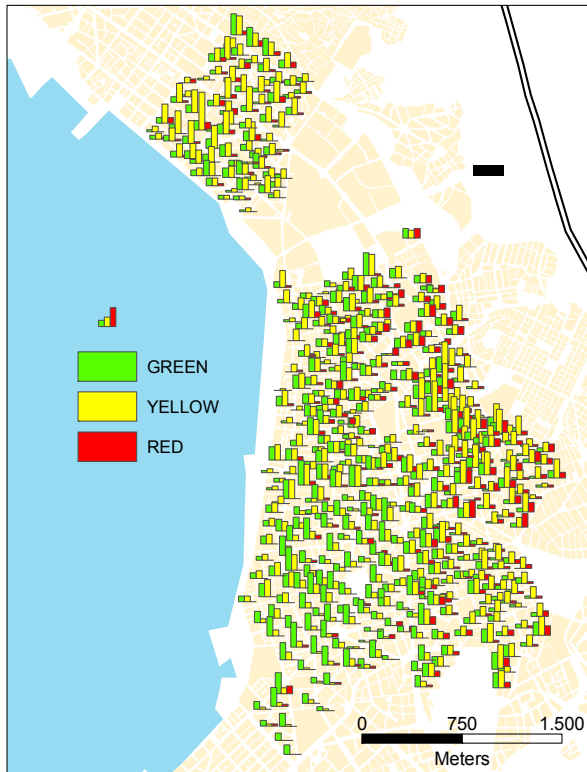


Fig. 15 Predicted tagging of buildings in each building block

Given the limitations of the procedure for assigning each individual building within a block to a discrete damage state, it is important to map also the damage index for each block, this time as a weighted one (by volume), as discussed previously; this puts the damage distribution ‘into scale’ in the sense that the degree of damage is now associated with the volume of the buildings (e.g. a collapsed single-storey masonry building has a smaller influence on the index than a 9-storey R/C building suffering “substantial to heavy” damage, i.e. DS3).

Last but not least, the economic loss predicted for the scenario earthquake is of particular importance, in several ways (earthquake protection and emergency planning, earthquake insurance). The fragility models developed by the AUTH group originate from repair cost considerations, hence it was relatively straightforward to use them for economic loss assessment purposes.

The map of Fig. 16 shows the estimated total cost of repair required in each building block, derived using the loss indices of Table 3 and assuming an average replacement cost of €700 /m<sup>2</sup>, i.e. calculating  $\Sigma[(V_i \cdot MDF_i) \cdot 700]$  in each block. The distribution of cost is, of course, consistent with (and conditional on) the distribution of the degree of damage. A very heavy cost of over 460 million € for the PGA-based, or 330million € for the  $S_d$ -based approach is predicted for the area studied (the figure should be multiplied by about 4 for the entire municipality), again an indication of the severity of the estimated scenario earthquake.

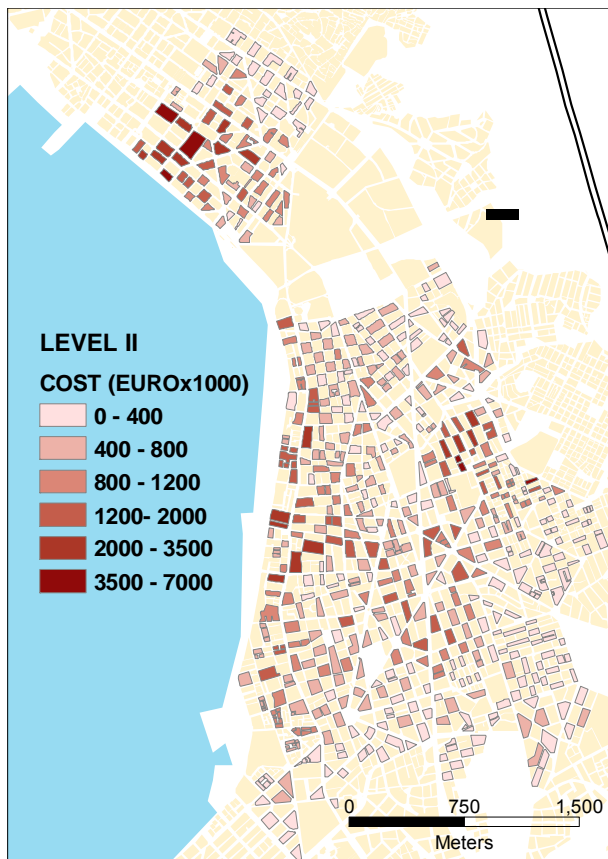


Fig. 16 Repair cost (in  $10^3\text{€}$ ) distribution in the building blocks of the studied area.

## 6 Concluding remarks

This chapter has tackled a number of issues relating to vulnerability and loss assessment, with particular emphasis on the situation in Greece and S. Europe. A classification scheme that is deemed appropriate for the building stock in this area has been proposed, aiming at an adequate description of the R/C buildings that currently dominate the built volume, without neglecting the case of URM buildings, which due to their higher vulnerability are often an important contributor to the future losses.

The key idea of AUTH's hybrid approach to seismic vulnerability assessment is the combination of damage statistics (empirical data) with results from inelastic analysis; this is an approach that clearly differs from most other procedures, among which the well-known procedure adopted by HAZUS, wherein fragility curves are based directly on inelastic (static) analysis, and the only empirical component in their derivation is the definition (by judgement) of the damage state thresholds. This chapter addressed both R/C and URM buildings, and made it clear that different analytical procedures are better suited to each case, given that URM buildings are still not very amenable to inelastic time-history analysis, which is, nevertheless, well-established for their R/C counterparts. Despite the different type of analysis used in each case, the hybrid component was used for both types of buildings and in both cases the key empirical parameter was the cost of repair of a damaged building; this is a particularly useful parameter, but reliable data is not always available on it, which means that other parameters (structural damage indices) could certainly be explored within the broader frame of the hybrid approach.

The procedure used for developing R/C building fragility curves based on the use of inelastic dynamic analysis, is the relatively more refined approach (again bearing in mind the major uncertainties involved at all steps of the analysis), but its cost is clearly higher than that of the simpler procedure used for URM buildings, based on inelastic static analysis and the ‘capacity spectrum’ approach.

The type of assumption made for the functional form of the fragility curve is also a key one, but the current trend world-wide seems to be towards adopting the lognormal cumulative distribution function; the determination of damage medians and the variabilities associated with each damage state can be done using the procedures described in HAZUS, or the alternative ones suggested herein. It is noted, though, that values of the variabilities proposed in HAZUS should not be adopted blindly if the analytical procedure used is not the one based on the ‘capacity spectrum’.

Regarding the two different types of fragility curves that can be used, PGA-based curves offer a number of advantages, but also ignore, to an extent that depends on the spectral characteristics of the motions considered for deriving the fragility curves and their relationship to the characteristics of the scenario motions, the possibly lower damageability of motions with high PGA and spectra peaking over a very narrow band and/or with very short duration (both these characteristics are more or less typical in strong motions recorded in Greece). The  $S_d$ -based curves take into account the spectral characteristics of the motion but further research is needed in several points such as the case where the capacity spectrum method does not result in a solution, or the equal displacement assumption is not valid.

Of particular practical relevance is the simple procedure suggested in section 4, based on the area under pseudovelocity spectra, for adapting fragility curve sets developed for a specific ground motion (be it a spectrum or a set of accelerograms) to the ground motion that is (more) representative of seismic hazard in another geographical area.

Finally, a specific application to the municipality of Thessaloniki was presented and the different types of scenario that can be developed using the aforementioned fragility curves were illustrated. It is within the scope of the work envisaged by the AUTH research group to improve the methodologies for assessing the vulnerability of both common and monumental structures, using damage information from past earthquakes in combination with nonlinear analysis of carefully selected representative structures.

## **7 Acknowledgements**

Most of the work reported in this chapter was carried out within the framework of three research projects, RISK-UE and SRM-DGC, funded by the European Commission, and ARISTION, funded by the General Secretariat of Research and Technology of Greece.

It should be clear from the material presented here that the vulnerability studies at AUTH have been a joint effort of the author and his colleagues, notably Prof. K. Stylianidis, and also a number of highly-motivated graduate students like G. Panagopoulos, Gr. Penelis, C. Panagiotopoulos, E. Papadopoulos, and K. Morfidis, to name just a few. The author also wishes to acknowledge the assistance of Prof. K. Pitilakis (AUTH) for making available data from microzonation studies carried out by his group.

## 8 References

- Anastasiadis, A., Raptakis, D., Pitilakis K. 2001. Thessaloniki's Detailed Microzoning: Subsurface Structure as basis for Site Response Analysis, *Pure and Applied Geophysics*, 158(12): 2597-2633.
- Applied Technology Council (ATC) 1985. Earthquake damage evaluation data for California (ATC-13) Appl. Technology Council, Redwood City, California.
- Applied Technology Council 1996. ATC-40: Seismic evaluation and retrofit of concrete buildings, Rep. SSC 96-01, CSSC-ATC, Redwood City, Calif.
- Athanassiadou, C., Lekidis, V., Kappos A. & Karakostas, C. 2007. Calibration of Eurocode 8 (EN1998-1) site-dependent acceleration and displacement spectra using records from Greece, *4<sup>th</sup> International Conference on Earthquake Geotechnical Engineering* (Thessaloniki June 25-28, 2007) Paper No. 1192.
- Athanassiadou, C.J., Karakostas, C.Z., Margaris, B.N., Kappos, A.J. 2011. Evaluation of design displacement spectra and displacement modification factors, on the basis of records from Greece. *Soil Dynamics & Earthquake Engineering*, 31(12), 1640-1653
- Barbat, A.H., Moya, F.Y., Canas, J.A., et al. 1996. Damage Scenarios Simulation for Seismic Risk Assessment in Urban Zones. *Earthquake Spectra* 12(3): 371-394.
- Bard, P.Y., et al. 1995. Seismic zonation methodology for the city of Nice-Progress report. *Proceedings 3rd Intern. Conf. on Seismic Zonation* (Nice, France), III: 1749-1784.
- Computers and Structures Inc. 2002. *SAP2000 – Version 8: Integrated software for structural analysis and design*, Berkeley, California.
- D'Ayala, D.F., Spence, R.J.S., Oliveira, C.S., & Silva, P. 1996. Vulnerability of buildings in historic town centres: A limit-state approach. *11th World Conference on Earthquake Engineering* (Acapulco, Mexico), Paper No. 864 [CD ROM Proceedings], Pergamon.
- Dolce, M., Kappos, A., Masi, A., Penelis, Gr. & Vona, M. 2006. Vulnerability assessment and earthquake damage scenarios of the building stock of Potenza (Southern Italy) using italian and greek methodologies. *Engineering Structures* 28 (3): 357-371.
- Dymiotis, C., Kappos A.J., and Chryssanthopoulos, M.C. 1999. Seismic reliability of R/C frames with uncertain drift and member capacity. *J. Str. Engng*, ASCE, 125(9): 1038-1047.
- Erdik, M., et al. 2003. Earthquake risk assessment for Istanbul metropolitan area, *Earthquake Engineering and Engineering Vibration* 2(1): 1-23.
- Faccioli E., Pessina V., Calvi, G.M., & Borzi, B. 1999. A study on damage scenarios for residential buildings in Catania city. *Journal of Seismology* 3(3): 327-343.
- Fardis, M.N., Karantoni, F. V., and Kosmopoulos, A. 1999. Statistical evaluation of damage during the 15-6-95 Aegio Earthquake, Final Report to the Sponsor (EPPO), Patras (in Greek).
- FEMA-NIBS 2003. Multi-hazard Loss Estimation Methodology - Earthquake Model: HAZUS®MH Technical Manual. Washington DC.
- Kappos, A.J. 2001. Seismic vulnerability assessment of existing buildings in Southern Europe, *Keynote lecture*, Convegno Nazionale 'L'Ingegneria Sismica in Italia' (Potenza/Matera, Italy), CD ROM Proceedings
- Kappos, A.J. and Panagopoulos, G. 2010. Fragility curves for R/C buildings in Greece. *Structure & Infrastructure Engineering*, 6(1), 39 – 53.
- Kappos, A.J., Panagopoulos, G., Panagiotopoulos, Ch. & Penelis, Gr. 2006. A hybrid method for the vulnerability assessment of R/C and URM buildings. *Bull. of Earthquake Engineering* 4 (4): 391-413.
- Kappos, A.J., Panagopoulos, G., and Penelis, Gr. 2008. Development of a seismic damage and loss scenario for contemporary and historical buildings in Thessaloniki. *Soil Dynamics & Earthq.Engng*, 28(10-11), 836-850.
- Kappos, A.J., G.K. Panagopoulos, A.G. Sextos, V.K. Papanikolaou, K.C. Stylianidis 2010. Development of Comprehensive Earthquake Loss Scenarios for a Greek and a Turkish City - Structural Aspects. *Earthquakes & Structures*, 1(2), 197-214

- Kappos, A., Pitilakis, K., Morfidis, K. & Hatzinikolaou, N. 2002. Vulnerability and risk study of Volos (Greece) metropolitan area. *12th European Conference on Earthquake Engineering* (London, UK), CD ROM Proceedings (Balkema), Paper 074.
- Kappos, A.J., Stylianidis, K.C., and Michailidis, C.N. 1998a. Analytical models for brick masonry infilled R/C frames under lateral loading, *Journal of Earthquake Engineering*, 2 (1): 59-88.
- Kappos, A.J., Stylianidis, K.C., and Pitilakis, K. 1998b. Development of seismic risk scenarios based on a hybrid method of vulnerability assessment. *Nat. Hazards*, 17(2): 177-192.
- Koliopoulos, P.K., Margaritis, B.N. and Klimis, N.S. 1998. Duration and energy characteristics of Greek strong motion records. *Journal of Earthquake Engineering* 2(3): 391-417.
- Lagomarsino, S. & Giovinazzi, S. 2006. Macroseismic and mechanical models for the vulnerability and damage assessment of current buildings, *Bull. of Earthquake Engineering*, 4 (4): 415-443.
- Penelis G.G. & A.J. Kappos 1997. *Earthquake-resistant Concrete Structures*. E&FN SPON (Chapman & Hall), London.
- Penelis, G.G., Sarigiannis, D., Stavrakakis, E. and Stylianidis, K.C. 1989. A statistical evaluation of damage to buildings in the Thessaloniki, Greece, earthquake of June, 20, 1978. *Proceedings of 9th World Conf. on Earthq. Engng.* (Tokyo-Kyoto, Japan, Aug. 1988), Tokyo:Maruzen, VII:187-192.
- Penelis, Gr.G. 2006. An efficient approach for pushover analysis of unreinforced masonry (URM) structures. *Jnl of Earthquake Engineering*, 10 (3): 359-379.
- Penelis, Gr.G., Kappos, A.J., Stylianidis, K.C., & Lagomarsino S. 2002. Statistical assessment of the vulnerability of unreinforced masonry buildings. *International Conference Earthquake Loss Estimation and Risk Reduction*, Bucharest, Romania.
- Pitilakis, K., et al. 2004. An advanced approach to earthquake risk scenarios with applications to different European towns: Synthesis of the application to Thessaloniki city, RISK-UE Report.
- Pitilakis, K. et al. (2011) Development of comprehensive earthquake loss scenarios for a Greek and a Turkish city: Seismic hazard, Geotechnical, and Lifeline Aspects. *Earthquake and Structures*, 2(3), 207-232.
- Spence, R.J.S., et al. 1992. Correlation of ground motion with building damage: The definition of a new damage-based seismic intensity scale, *Proceed. 10th World Conf. on Earthq. Engng.* (Madrid, Spain) Balkema, Rotterdam, Vol. 1, 551-556.